1α,25-Dihydroxyvitamin D_3 and Its TX527 Analog Inhibit the Growth of Endothelial Cells Transformed by Kaposi Sarcoma-Associated Herpes Virus G Protein-Coupled Receptor *in Vitro* and *in Vivo*

Verónica Gonzalez-Pardo, Daniel Martin, J. Silvio Gutkind, Annemieke Verstuyf, Roger Bouillon, Ana Russo de Boland, and Ricardo L. Boland

Departamento de Biología Bioquímica y Farmacia (V.G.-P., A.R.d.B., R.L.B.), Universidad Nacional del Sur. San Juan 670, 8000 Bahía Blanca, Argentina; Cell Growth Regulation Section (D.M., J.S.G.), Oral and Pharyngeal Cancer Branch, National Institute of Dental and Craniofacial Research, National Institutes of Health, Bethesda, Maryland 20892; and Laboratorium voor Experimentele Geneeskunde en Endocrinologie (A.V., R.B.), Katholieke Universiteit Leuven, B-3000 Leuven, Belgium

The Kaposi sarcoma-associated herpes virus-G protein-coupled receptor is a key molecule in the pathogenesis of Kaposi sarcoma, playing a central role in promoting vascular endothelial growth factor-driven angiogenesis and spindle cell proliferation. We studied the effects of 1α,25-dihydroxyvitamin D_3 [1α,25$(OH)_2D_3$] and the analog TX527 on the proliferation of endothelial cells (SVECs) and SVECs transformed by the viral G protein-coupled receptor (SVEC-vGPCR). 1α,25$(OH)_2D_3$ and TX527 decreased SVEC-vGPCR and SVEC numbers, the response being time dependent and similar in both cell lines. Vitamin D receptor (VDR) levels increased on treatment with 10 nM 1α,25$(OH)_2D_3$ or 1 nM TX527 in a time-dependent manner (1.5–24 h) in SVECs and SVEC-vGPCR. Basal VDR levels were increased in SVEC-vGPCR. The antiproliferative effects were accompanied by reduction in cyclin D1 and accumulation of p27 in SVECs but not SVEC-vGPCR. Induction of VDR was blocked by transfection of short hairpin RNA against VDR in SVEC-vGPCR and the antiproliferative effects of 1α,25$(OH)_2D_3$ and TX527 were decreased, involving the VDR genomic pathway in the hormone and analog mechanism of action. *In vivo* experiments showed that 1α,25$(OH)_2D_3$ and TX527 decreased SVEC-vGPCR tumor progression when the tumor cells were implanted in nude mice. In conclusion, we have demonstrated that 1α,25$(OH)_2D_3$ and its TX527 analog have antiproliferative effects on the growth of endothelial cells transformed by the vGPCR *in vitro* and *in vivo*, the vitamin D receptor being part of the inhibitory mechanism of action. **(*Endocrinology* 151: 23–31, 2010)**

1α,25-dihydroxyvitamin D_3 [1α,25$(OH)_2D_3$] plays an essential role in the regulation of calcium homeostasis, cell proliferation, and differentiation and in the immune system (1). More recently its ability to induce apoptosis, inhibit angiogenesis, tumor invasion and metastasis, and modulate cytokine production has been demonstrated (2). Similarly as other steroid hormones, 1α,25$(OH)_2D_3$ elicits responses through both nuclear receptor [vitamin D receptor (VDR)]-mediated gene transcription and a fast mechanism independent of new RNA and protein synthesis with activation of second-messenger pathways (3, 4). In most cell types, the antiproliferative effect of 1α,25$(OH)_2D_3$ results in an accumulation of cells in the G_0/G_1 phase of the cell cycle. Different signaling pathways are involved and converge at the level of complex formation between the retinoblastoma family of pocket proteins, the electro-acoustic 2 factor (E2F) family of transcription factors and the subsequent down-regulation of

ISSN Print 0013-7227 ISSN Online 1945-7170
Printed in U.S.A.

doi: 10.1210/en.2009-0650 Received June 11, 2009. Accepted October 20, 2009.
First Published Online November 13, 2009

Abbreviations: HHV8, Human herpes virus 8; KS, Kaposi sarcoma; NF-κB, nuclear factor-κB; 1α,25$(OH)_2D_3$, 1α,25-dihydroxyvitamin D_3; shmVDR, shRNA against mouse VDR; shRNA, small hairpin RNA; SVEC, Simian virus 40 immortalized murine endothelial cell; TdT, terminal deoxynucleotidyl transferase; VDR, vitamin D receptor; vGPCR, viral G protein-coupled receptor.

E2F-target genes that are required for normal cell cycle progression. The pocket proteins p107 and p130 are crucial to the antiproliferative activity of 1α,25(OH)$_2$D$_3$ (5). Activation of cyclin-dependent kinase inhibitors p18, p19, p21, or p27 and repression of cyclin D1 expression as well as down-regulation of the activity of complexes between cyclins and cyclin-dependent kinases have been suggested to be early events, whether or not directly mediated by 1α,25(OH)$_2$D$_3$, that occur upstream of the E2F pathway and may be responsible for the growth-inhibitory effect of 1α,25(OH)$_2$D$_3$. However, 1α,25(OH)$_2$D$_3$ may also inhibit cell growth by interfering with signaling pathways initiated by TGFβ, epithelial growth factor, IGF, prostaglandins, and Wnt-ligands as well as by intervening in other mitogenic signaling pathways (6).

Kaposi sarcoma (KS) is a highly vascular tumor, and the tumor cells display features of activated endothelial cells, including high expression of several phenotypic markers and various specific tyrosine kinases (7). It has been shown that the tumor cells produce and respond to several factors, including IL-1, IL-6, IL-8, oncostatin-M, vascular endothelial growth factor and basic fibroblast growth factor. Other studies suggest that the human herpes virus 8 (HHV8; also known as KS herpesvirus) would be involved in KS development (8, 9). Furthermore, transgenic expression of viral G protein-coupled receptor (vGPCR), the constitutively active chemokine receptor encoded by HHV8, induced angiogenic lesions similar to those observed in human KS lesions (10, 11).

The potential effect of 1α,25(OH)$_2$D$_3$ and its TX527 analog as therapeutic strategy for KS treatment has not been fully established. It has been shown that KS responds to 1α,25(OH)$_2$D$_3$, *e.g.* KS cell growth rate in culture and tumor xenograft growth in nude mice are inhibited by the hormone. A mechanism for the antineoplastic effect of 1α,25(OH)$_2$D$_3$ in SK that involves the inhibition of the expression of IL-6 and IL-8 has been suggested (7). However, transient expression analysis revealed that the promoter involved in down-regulation of IL-6 transcription by 1α,25(OH)$_2$D$_3$ is devoid of the VDR response element to which a heterodimer of the VDR and retinoid X receptor binds to modulate expression of target genes (7).

Based on the antineoplastic activity reported for 1α,25(OH)$_2$D$_3$ in several tumor types and due to scarce knowledge concerning the mechanisms involved therein, the aim of this work was to study the effects of 1α,25(OH)$_2$D$_3$ and its less calcemic analog TX527 on the proliferation of endothelial cells transformed by the vGPCR *in vitro* and *in vivo* and to investigate whether the VDR is involved in the mechanism of action of both compounds.

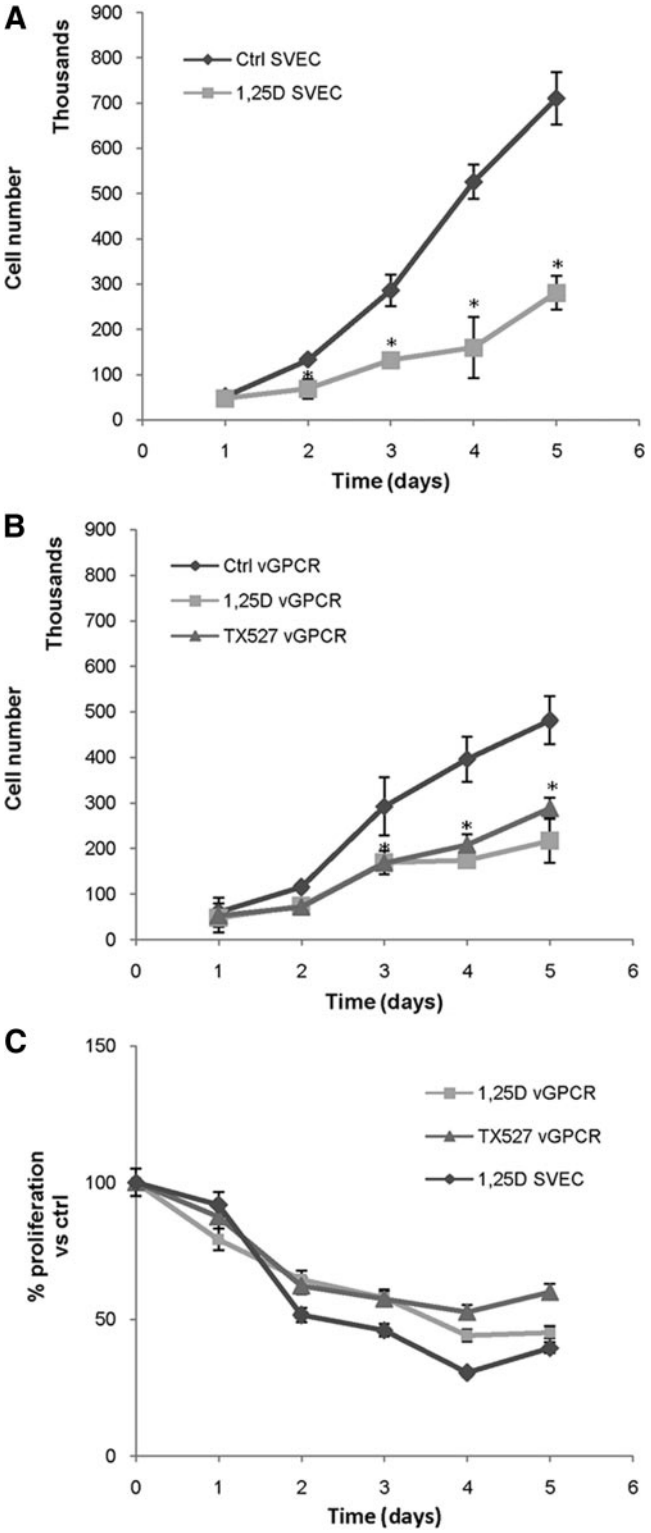

FIG. 1. Effect of 1α,25(OH)$_2$D$_3$ and its analog TX527 on growth of SVECs and SVEC-vGPCR cells. Both cells lines were seeded in 12-well plates at 10,000 cells/well. After overnight growth, the cells were treated with 10 nM 1α,25(OH)$_2$D$_3$ (1,25D) and 1 nM TX527 or vehicle isopropanol (Ctrl, control) in DMEM 10% serum for 1–5 d. A and B, Cell counts were performed in a Neubauer chamber at the day selected. The data from each experiment are means ± SD performed in triplicate. Significant differences between control and treated conditions are indicated. *, $P < 0.05$. C, Data were expressed as percentage of inhibition respect to control and are representative of three independent experiments.

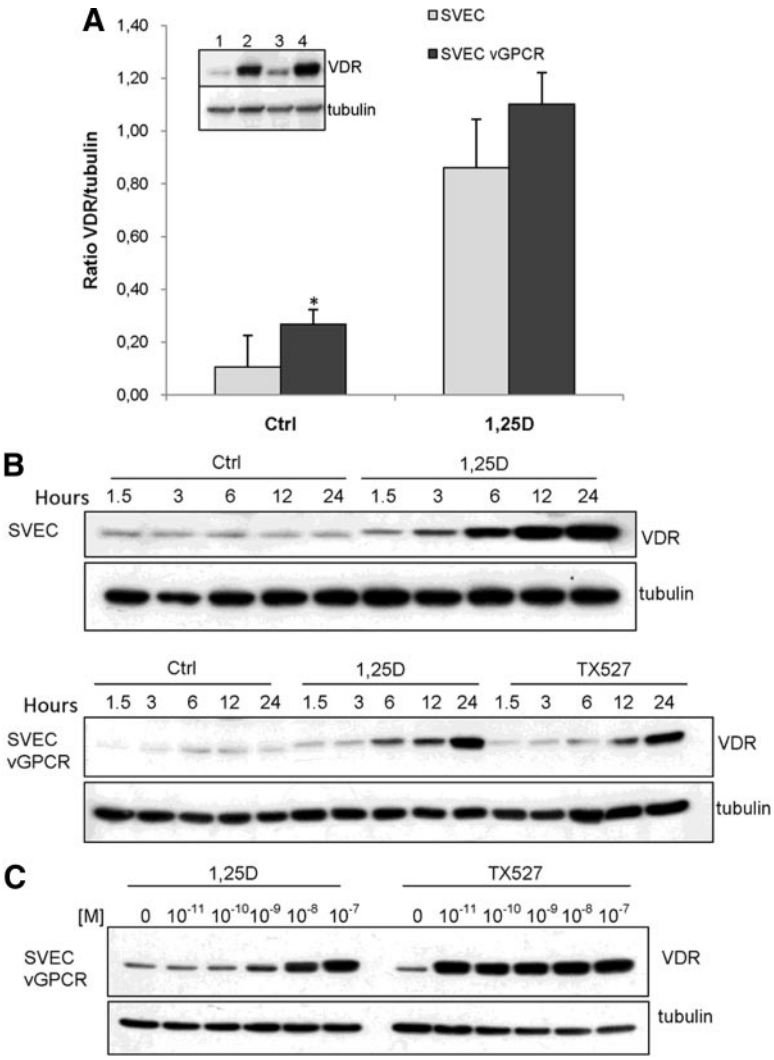

FIG. 2. $1\alpha,25(OH)_2D_3$ and TX527 induce the expression of VDR in SVECs and SVEC-vGPCR cells. SVECs and SVEC-vGPCR were plated at 70% confluence and 24 h later were treated with 10 nM $1\alpha,25(OH)_2D_3$ (1,25D) for 24 h (A), 10 nM $1\alpha,25(OH)_2D_3$ (1,25D), or 1 nM TX527 for 1.5–24 h (B) and 10^{-11} to 10^{-7} M $1\alpha,25(OH)_2D_3$ (1,25D), or TX527 for 24 h (C). Cell lysates were prepared and subjected to Western blot analysis with anti-VDR and anti-tubulin as described in *Materials and Methods*. A, SVEC: lanes 1 (Ctrl, control) and 2 ($1\alpha,25(OH)_2D_3$); SVEC-vGPCR: lanes 3 (control) and 4 [$1\alpha,25(OH)_2D_3$]. The bands were quantified by densitometry and the ratios between VDR and tubulin levels were taken into account for statistical analysis. *, $P < 0.05$. The data shown are representative of five independent experiments.

Materials and Methods

Chemicals and reagents

$1\alpha,25(OH)_2D_3$ and the 19-nor-14,20-bisepi-23-yne-$1,25(OH)_2D_3$ analog (TX527), originally synthesized by M. Vandewalle and P. De Clercq (University of Ghent, Ghent, Belgium), were provided by Théramex (Monaco). Immobilon P (polyvinylidene difluoride) membranes were from Sigma-Aldrich (St. Louis, MO). The antibodies used were monoclonal anti-VDR (Affinity Bioreagents, Golden, CO), anti-cyclin D1 (Neomarkers, Fremont, CA), anti-p27, antitubulin, and polyclonal anti-VDR as well as antirabbit, antimouse, and antirat horseradish peroxidase-conjugated secondary antibodies (Santa Cruz Biotechnology, Santa Cruz, CA). For most applications, $1\alpha,25(OH)_2D_3$ was used at 10 nmol/liter because this concentration consistently shows antiproliferative effects in multiple assays in a variety of tumor cell types. For *in vivo* experiments the compounds were diluted in Arachis oil (Sigma-Aldrich). Other chemicals used were of analytical grade.

Cell lines and transfections

Simian virus 40 immortalized murine endothelial cells (SVECs) stably expressing vGPCR full-length (pCEFLvGPCR) or empty vector (pCEFL) as a control were used. Stable overexpression of vGPCR promotes tumor formation when these cells are injected into immunosuppressed mice and induces angiogenic lesions similar to those developed in KS (10). Transfected cells were selected with 750 μg/ml G418 (Cellgro, Manassas, VA).

Infection with lentivirus particles

Stable SVEC-vGPCR endothelial cells targeted with small hairpin RNA (shRNA) against mouse vitamin D receptor (shmVDR) or control shRNA were infected with lentiviral particles generated in HEK293T cells following the manufacturer's protocols. The plasmid to knock down the VDR was PLKO.1, clone ID TRCN0000027101 (Open Biosystems, Huntsville, AL). The stable cell line was selected with 2 μg/ml puromycin (Invivogen, San Diego, CA) and the medium was freshly changed every other day. VDR knockdown was monitored by Western blot analysis and was achieved after five passages.

Proliferation assays

Cells were seeded in 12-well plates, at 10,000 cells/well. After overnight growth, the cells were treated with $1\alpha,25(OH)_2D_3$, TX527, or vehicle in triplicate in DMEM-10% fetal bovine serum for 1–5 d. Medium and compounds were replaced every other day. The cells were harvested and counted in a Neubauer chamber at the day selected. Alternatively, the cells were spun down and lysed for Western blot analysis as indicated below.

SDS-PAGE and Western blot analysis

Whole-cell lysates from cultures treated with $1\alpha,25(OH)_2D_3$ or TX527 as indicated for each experiment were prepared as previously described (12). Protein content was determined by the Bradford method (13). Samples were resolved by SDS-PAGE and transferred overnight to polyvinylidene difluoride membranes. Western blot analyses were performed as reported before (12). Antibodies used include monoclonal anti-VDR (1:1500), anti-cyclin D1 (1:500), and anti-p27 (1:500) and antitubulin (1:1500) combined with antirabbit (1:10,000), antimouse (1:5,000), or antirat (1:5,000) horseradish peroxidase-conjugated secondary antibodies.

Tumor allografts in athymic (nu/nu) nude mice and *in vivo* treatment

Animal studies were carried out according to the National Institutes of Health animal care and user protocol. SVEC-

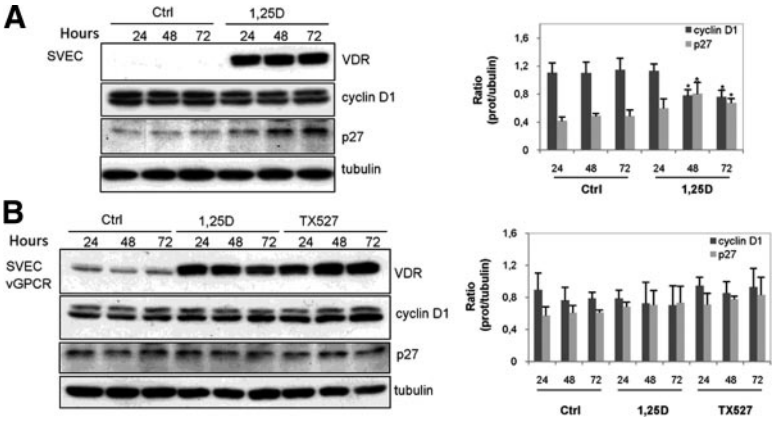

FIG. 3. Differential effects of 1α,25(OH)$_2$D$_3$on VDR, cyclin D1, and p27 in SVECs and SVEC-vGPCR cells. Both endothelial cell lines were plated at 50% and 24 h later were treated with 10 nM 1α,25(OH)$_2$D$_3$ or TX527 or vehicle for 24–72 h. Whole-cell lysates were prepared and subjected to Western blot analysis with anti-VDR, anti-cyclin D1, anti-p27, and anti-tubulin. A, SVEC cells. B, SVEC-vGPCR cells. Cyclin D1 and p27 bands were quantified by densitometry and the ratios between the proteins and tubulin levels were taken into account for statistical analysis. *, $P < 0.05$. The data shown are representative of three independent experiments. Ctrl, Control.

vGPCR cells were used to induce allografts in 6-wk-old athymic (nu/nu) female's nude mice as described elsewhere (10). Exponentially growing cells were harvested, resuspended in DMEM, and 1×10^6 viable cells injected sc in the right/left flank of the mouse. The animals were monitored two times weekly for tumor formation. Tumors were noticeable and reached a diameter of approximately 4 mm after 20 d of cell injection. Tumor-bearing animals were randomly grouped (n = 5) and treated with arachis oil (group 1, control), 1α,25(OH)$_2$D$_3$ (5 μg/kg/d, group 2), and TX527 (10 μg/kg/d, group 3) dissolved in equal volume of arachis oil, administered by ip injection for 4 consecutive days. Tumor volume and body weight were measured every other day during the period of investigation (22 d). Tumor size was determined by measuring the length and width and tumor volume was calculated with the formula, volume = $(L \times W^2)/2$. L and W represent longest length and shortest width of the tumor. Results were expressed as mean ± SE. At the end of the study interval, the animals were euthanized for tissue retrieval; the tumors were weighed and fixed for immunohistochemical analysis.

In vivo calcemic activity of compounds

The calcemic effects of 1α,25(OH)$_2$D$_3$ and its TX527 analog were monitored after completion of the *in vivo* experiments. Serum calcium was measured using an ion selective electrode method in the Department of Laboratory Medicine, National Institutes of Health (Bethesda, MD).

Immunohistochemistry

For immunohistochemical staining, tissues were fixed in 4% paraformaldehyde/1× PBS overnight, transferred to 70% ethanol/PBS, and embedded in paraffin. Sections were cleared in a graded xylene/ethanol series. Antigens were retrieved and then washed in PBS. To block endogenous peroxidase, the sections were treated with 3% hydrogen peroxide/H_2O_2 for 10 min, washed with PBS, and then incubated with anti-Ki67 proliferation marker antibody in DakoCytomation buffer diluent (Tecnolab, Buenos Aires, Argentina) for 1 h at room temperature. Control sections were incubated with buffer diluent alone. After three washes for 5 min with PBS, the sections where incubated with Dako envision system peroxidase (Tecnolab) 45 min at room temperature. The peroxidase activity was developed using 3–3 diaminobenzidine as a substrate. Slides were counterstained with hematoxylin, dehydrated, and mounted with Permount (Fisher Scientific, Fair Lawn, NJ). Positive Ki67 nuclei were counted in ten fields with a ×40 objective by different observers.

Terminal deoxynucleotidyl transferase (TdT)-mediated deoxyuridine triphosphate nick end labeling assay

Paraffin sections were dewaxed by heating the slides at 60 C followed by washing in xylene and rehydration through a graded series of ethanol. The slides were stored in 70% ethanol for 48 h at −20 C. Before labeling, slides were washed twice with PBS for 5 min at room temperature. Samples were preincubated with 1× TdT buffer for 15 min and then incubated with the TdT reaction mixture (0.05 mM bromodeoxyuridine triphosphate, 0.3 U/μl TdT in TdT buffer) at 37 C in a humidified atmosphere for 1 h. The reaction was stopped 15 min incubation with stop buffer [300 mM NaCl, 30 mM sodium citrate (pH 7.4)] at room temperature. Negative controls were prepared by omitting TdT. 5-Bromo-2′-deoxyuridine presence was determined with anti-5-bromo-2′-deoxyuridine monoclonal antibody, following a standard immunocytochemical technique.

Statistical analysis

Data are shown as means ± SD. Statistical differences between mean serum calcium levels of experimental groups were calculated by the two-tailed *t* test. A $P < 0.01$ (**) and < 0.05 (*) was considered highly statistically significant and statistically significant, respectively. Data from cell growth, tumor volumes, and weights were first analyzed with one-way ANOVA for each day of the experimental period. This analysis was followed by application of the multiple comparison Bonferroni test to compare means.

Results

1α,25(OH)$_2$D$_3$ and TX527 inhibit endothelial cell growth *in vitro*

The growth-regulatory effects of VDR agonists on endothelial cells were tested using the SVECs (pCEFL, control cells) and SVECs stably transfected with the viral receptor of herpes virus 8 (SVEC-vGPCR), a cellular model of KS. After treatment of cultures with 1α,25(OH)$_2$D$_3$ or its synthetic analog TX527, cell numbers were measured using a microscope counting chamber. The results presented in Fig. 1, A and B, demonstrated that 1α,25(OH)$_2$D$_3$ inhibits the proliferation of both endothelial cell lines in a time-dependent fashion, SVECs being slightly more sensitive to the hormone than vGPCR cells (Fig. 1C). TX527 also inhibited the growth of SVEC-

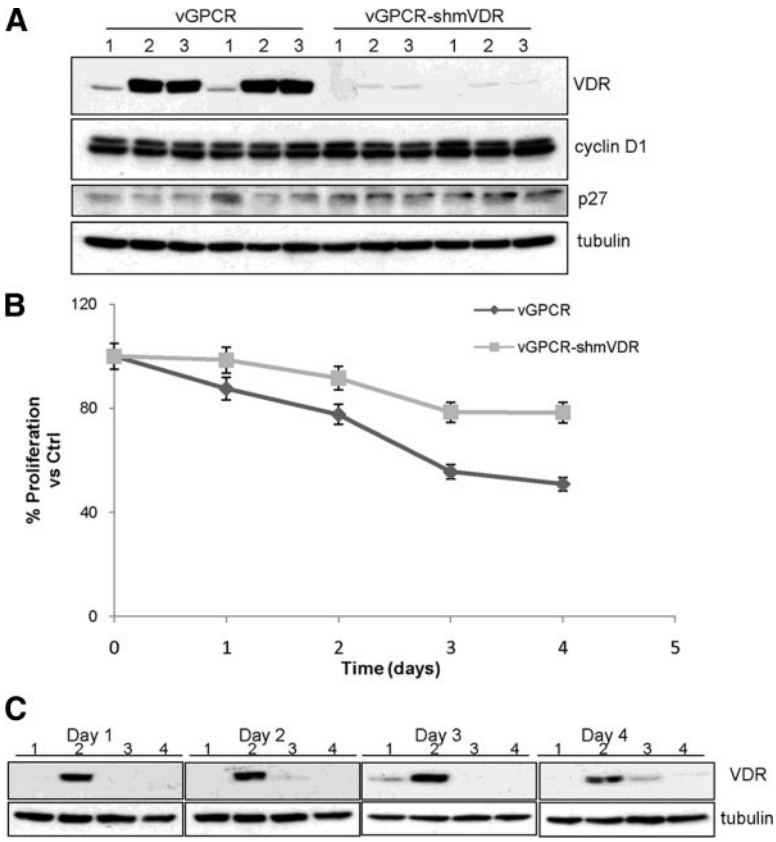

FIG. 4. Targeted VDR knockdown impairs the ability of $1\alpha,25(OH)_2D_3$ and its analog TX527 to increase VDR levels and inhibit proliferation of SVEC-vGPCR cells. A, Established SVEC-vGPCR cell lines carrying control shRNA (vGPCR) and shmVDR (vGPCR-shmVDR) were plated at 70% confluence and 24 h later were treated with vehicle (lane 1), 10 nM $1\alpha,25(OH)_2D_3$ (lane 2), or TX527 (lane 3) for 48 h. Western blot analyses were performed for VDR, cyclin D1, p27, and tubulin. Duplicate blots for vGPCR and vGPCR-shmVDR representative of four independent experiments are shown. B, vGPCR and vGPCR-shmVDR cells were seeded at 10,000 cells/well. After overnight growth, the cells were treated with 10 nM $1\alpha,25(OH)_2D_3$ or vehicle for 1–4 d. Cell numbers were determined in a Neubauer chamber each day as described in *Materials and Methods*. The data were expressed as percentage of proliferation respect to control and are representative of three independent experiments. C, Whole-cell lysates from the preceding experiments were subjected to Western blot analysis to monitor VDR expression. The equivalence of protein loading was tested with antitubulin antibody. vGPCR, lane 1, control; lane 2, $1\alpha,25(OH)_2D_3$; vGPCR-shmVDR, lane 3: control; lane 4, $1\alpha,25(OH)_2D_3$.

vGPCR to the same extent as $1\alpha,25(OH)_2D_3$ but at 10-fold lower concentration (1 nM), showing a superagonist action. These results were confirmed by the 3-(4,5-dimethylthiazol-2-yl)-5-(3-carboxymethoxyphenyl)-2-(4-sulfophenyl)-2H-tetrazolium, inner salt assay (data not shown).

Expression of VDR in SVECs and SVEC-vGPCR cells

Variations observed in the proliferation of endothelial cells to $1\alpha,25(OH)_2D_3$ could be accounted for by differences in VDR expression (14). To investigate this possibility, VDR levels were evaluated by Western blot analysis in the SVEC and SVEC-vGPCR cell lines after treatment with 10 nM $1\alpha,25(OH)_2D_3$ for 1.5–24 h. Although higher basal VDR concentrations were detected in SVEC-vGPCR than SVECs under control conditions, treatment with $1\alpha,25(OH)_2D_3$ increased VDR protein expression in both cell lines (Fig. 2A) and with a similar time profile (Fig. 2B). Compound TX527 was also able to induce VDR protein expression in SVEC-vGPCR cells at a 10-fold lower concentration (Fig. 2B). A detailed dose-response study treating the vGPCR transfected endothelial cells with 10^{-11} to 10^{-7} M $1\alpha,25(OH)_2D_3$ and TX527 for 24 h confirmed that at 10^{-11} M the hormone did not modify VDR basal levels, whereas the analog increased receptor concentration more than 10-fold (Fig. 2C). Of interest, it has been reported that altered VDR binding to coactivators is one possible explanation for the superagonistic profile of the 14-epi-analog TX527 on cell proliferation (15).

Differential expression of cell cycle markers in response to $1\alpha,25(OH)_2D_3$

Differential antiproliferative effects of $1\alpha,25(OH)_2D_3$ on tumor-derived and matrigel endothelial cells reflected in specific cell cycle patterns have been reported (16). To test whether this differential response was due to differential expression of cell cycle markers, time-response studies (24–72 h) using $1\alpha,25(OH)_2D_3$ were carried out in both endothelial cell lines and VDR, cyclin D1, and p27 levels were analyzed by Western blot. As observed before, the hormone increased VDR levels in a time-dependent manner up to 72 h treatment (Fig. 3, A and B). In SVECs this response was accompanied by a reduction in cyclin D1 protein levels and an accumulation of p27 monitored by immunoblot analysis. Surprisingly, despite the fact that VDR expression was induced as predicted, cyclin D1, and p27 remained unaffected by $1\alpha,25(OH)_2D_3$ or TX527 treatment in the endothelial vGPCR cells (Fig. 3B), suggesting that other pathways are involved in the antiproliferative effects of $1\alpha,25(OH)_2D_3$ and TX527.

Targeted knockdown of VDR expression impairs $1\alpha,25(OH)_2D_3$-reduced cell proliferation

To determine whether $1\alpha,25(OH)_2D_3$ and its TX527 analog elicit their inhibitory growth effect through the VDR, lentivirus particles carrying shmVDR sequence were produced. First, the cells were infected with the lentiviral particles carrying control shRNA (vGPCR) and shmVDR (vGPCR-shmVDR). VDR knockdown was achieved after five passages monitored by Western blot

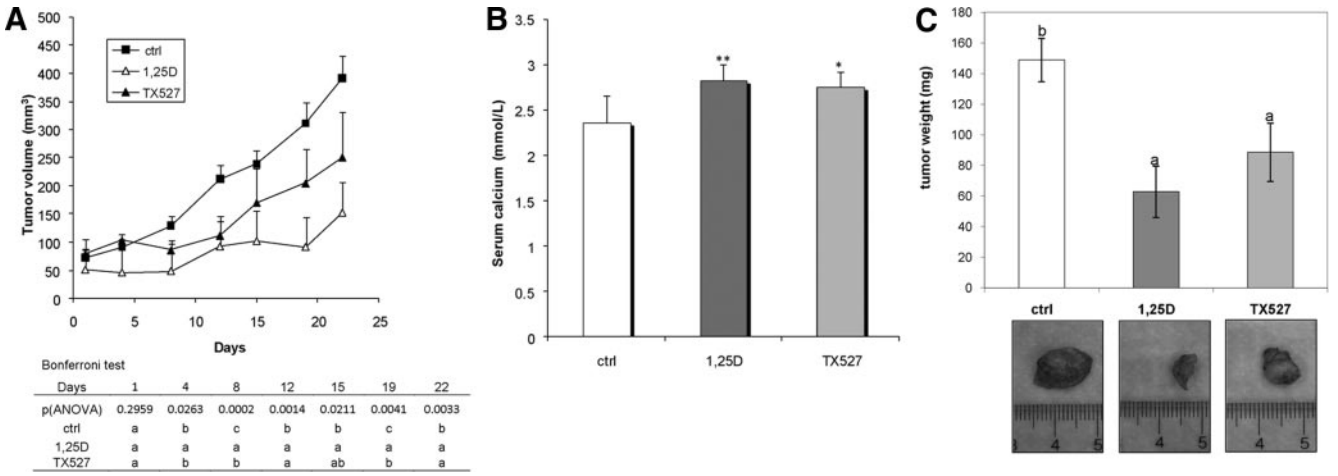

FIG. 5. *In vivo* antiproliferative effects of 1α,25(OH)$_2$D$_3$ and analog TX527. SVEC-vGPCR endothelial cells were used to establish allografts in athymic nu/nu mice. A, Evolution of tumor volume during the times indicated after tumor bearing nude female animals were treated with arachis oil as vehicle (■), 5 μg/kg·d 1α,25(OH)$_2$D$_3$ (1,25D) (△), and 10 μg/kg/d TX527 (▲) during 4 consecutive days. The data shown are the average of tumor volume of 10 tumors/group ± SE. The table shows the results of Bonferroni test for mean comparison. *Same letters for experimental groups* indicate $P > 0.05$, whereas *different letters* indicate $P < 0.05$. B, Serum calcium measured at the end of the *in vivo* experiment as described in *Materials Methods*. Values represent the average of five mice/group ± SD. Significant differences between control and treated animals are indicated. **, $P < 0.01$; *, $P < 0.05$. C, Tumors were dissected from SVEC-vGPCR endothelial cell allografts 26 d after treatment and their weights compared. The data are the average ± SD. Bonferroni test was used to determine the difference between 1α,25(OH)$_2$D$_3$/TX527 and control [*P* (ANOVA) = 0.001646].

analysis (Fig. 4A). To test whether 1α,25(OH)$_2$D$_3$ or TX527 was still able to induce VDR protein expression in stable VDR knockdown cells, control and knockdown cells were treated with 10 nM 1α,25(OH)$_2$D$_3$ and TX527 for 48 h. As shown in Fig. 4A (lanes 2 and 3), both compounds induced VDR expression in vGPCR cells, and this response was suppressed by stable knockdown of VDR (vGPCR-shmVDR cells). In agreement with the previous results (Fig. 3), cell cycle markers cyclin D1 and p27 remained unaltered in vGPCR and vGPCR-shmVDR cells (Fig. 4, lanes 1–3). Again, 1α,25(OH)$_2$D$_3$ inhibited the proliferation of vGPCR cells in a time-dependent manner (Fig. 4B) with maximum effect after 4 d treatment (51% respects to the control). Despite the fact that VDR knockdown was stable during duration of the experiment, and its expression was not detected by Western blot analysis (Fig. 4C), a very small decrease in proliferation was observed upon 1α,25(OH)$_2$D$_3$ treatment in VDR knockdown vGPCR-shmVDR cells after 3 and 4 d of hormone exposure, confirming that nearly all effects of 1α,25(OH)$_2$D$_3$ on cell proliferation are VDR mediated.

1α,25(OH)$_2$D$_3$and analog TX527 inhibit endothelial cell growth *in vivo*

To study whether 1α,25(OH)$_2$D$_3$ and TX527 also inhibit tumor progression *in vivo*, an experimental model for KS previously developed in mice (10) was established. Endothelial vGPCR cells were injected sc in the right/left flank of female nude mice. After tumor formation, animals were divided randomly into groups of five and they were treated with both compounds and vehicle for 4 consecutive d. 1α,25(OH)$_2$D$_3$ and TX527 were given the highest tolerable dose (5 and 10 μg/kg·d, respectively) and tumor development was followed during 22 d (Fig. 5A). Drug toxicity, as assessed by animal weight loss, was minimal in the 1α,25(OH)$_2$D$_3$- and TX527-treated groups (reduction < 10%) during the period of study (results not given). As shown in Fig. 5A, both 1α,25(OH)$_2$D$_3$ and TX527 retarded tumor development compared with control animals. Tumor regression in treated animals was observed for 22 d after beginning of the treatment, inhibition of tumor growth being sustained during the whole experiment. No significant reduction of body weight was detected during this study. In addition, no statistically significant differences between the effects of 1α,25(OH)$_2$D$_3$ and TX527 on serum calcium levels were found. Nonetheless, the calcemic activity of TX527 compared with control animals was significantly lower than 1α,25(OH)$_2$D$_3$ ($P < 0.05$ *vs.* $P < 0.01$, respectively) (Fig. 5B). At the end of the study (26 d), animals were euthanized and the tumors were removed and weighed. As shown in Fig. 5C, a highly significant reduction in tumor weight was observed in 1α,25(OH)$_2$D$_3$ and TX527-treated animals compared with the control group. To test whether tumor reduction correlates with cell growth inhibitory response, immunohistochemical staining of tumors (control and treated) with the proliferative marker Ki67 was performed (Fig. 6). The average of total positive Ki67 nuclei counted by different observers in 10 fields of ×40 objective was considered for statistical analysis. A statistically significant reduction in proliferation was observed in tumors treated

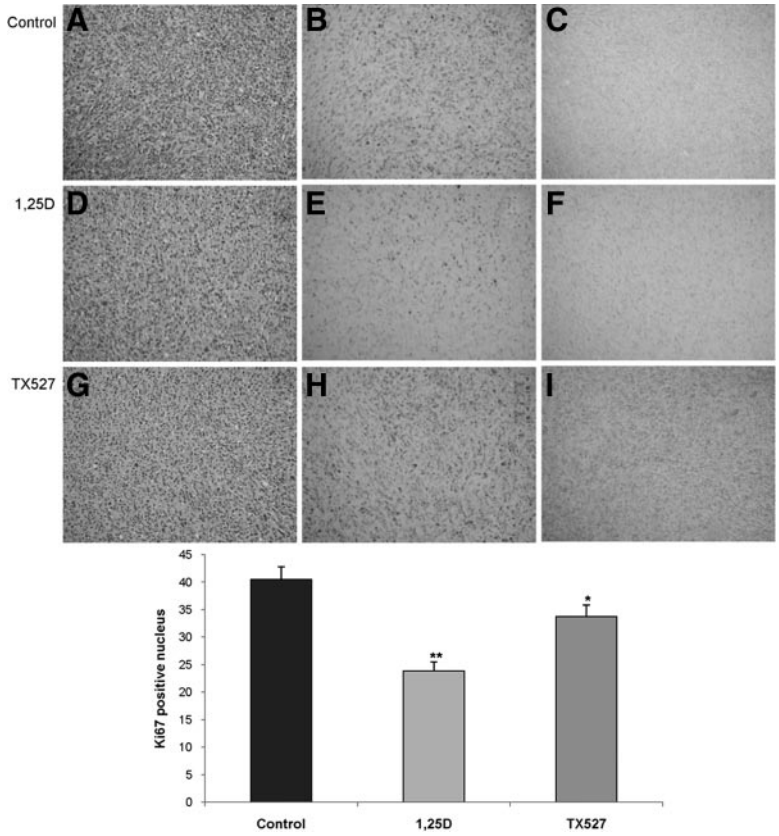

FIG. 6. Immunohistochemical analysis of tumors. Immunohistochemical staining of tumor sections was performed as described in *Materials and Methods*. A, D, and G, Hematoxylin and eosin staining to show experimental KS and tumor morphology. B, E, and H, Positive Ki67 nuclei counted in 10 fields of ×40 objective by different observers. C, F, and I, Control cells incubated with buffer alone. *Bar graph* represents mean ± SD. Student's *t* test was used to determine the difference between $1\alpha,25(OH)_2D_3$ (**, $P < 0.01$) and TX527 (*, $P < 0.05$) with respect to control.

with $1\alpha,25(OH)_2D_3$ (**, $P < 0.01$) and TX527 (*, $P < 0.05$) with respect to control, which is consistent with the data obtained in *in vitro* proliferation studies. Because $1\alpha,25(OH)_2D_3$ has been shown to promote apoptosis in various cell types, we explored whether the observed reduction in cell growth would be associated with apoptotic events. Neither $1\alpha,25(OH)_2D_3$ nor TX527 analog was able to induce DNA strand breaks in tissue sections as investigated by TdT-mediated deoxyuridine triphosphate nick end labeling (data not shown).

Discussion

The discovery of HHV8 as the viral etiologic agent of KS has unveiled many potential therapeutic targets (17). Numerous *in vitro* and *in vivo* studies have shown that $1\alpha,25(OH)_2D_3$ potently inhibits proliferation of a wide range of cell types (18, 19). Preclinical data suggested that $1\alpha,25(OH)_2D_3$ (alone or in combination with other agents) has potential applications in cancer prevention and treatment (2). However, because of its calcemic effects such as hypercalcemia, hypercalciuria, and increased bone resorption, the use of the hormone with therapeutic purposes is limited (20). Several analogs have been synthesized and evaluated, some of which display the desired dissociation between beneficial antiproliferative and unwanted calcemic effects. A number of these analogs are superagonistic and have a severalfold stronger antiproliferative action than the parent compound (15, 20, 21). The biological activity of two novel 14-epi-analogs TX522 [19-nor-14-epi-23-yne-$1\alpha,25(OH)_2D_3$] and TX527 [19-nor-14,20-bisepi-23-yne-$1,25(OH)_2D_3$] has been tested, demonstrating their ability to inhibit the growth of human breast cancer in animal models and in *vitro* by a mechanism that involves G_1 arrest and modulation of cyclin C and D1. According to these studies, apoptosis is not the major mechanism responsible for growth- inhibitory effects in MCF7 cells (15, 22). Based on the antineoplastic activity reported for $1\alpha,25(OH)_2D_3$ and its TX527 analog, in this work we studied the effects of both compounds on the proliferation of SVEC-vGPCR.

Our results demonstrated that both steroids have the ability to inhibit the growth of endothelial cells *in vitro* and *in vivo*; however, the less calcemic TX527 analog exerted its growth-inhibitory effects at a 10-fold lower concentration than the hormone. Moreover, data were obtained indicating that differential expression of the VDR in SVEC and SVEC-vGPCR cells may account for the differential reactivity of the cells to the compounds. In addition, VDR was up-regulated when the cells were treated with $1\alpha,25(OH)_2D_3$ and TX527. In this regard, expression of the VDR has been found to differentially increase in many cancer cells and tumors (23). Furthermore, supporting our data, VDR is expressed in other endothelial cell lines and tumor cells, and its ability to inhibit cell growth and angiogenesis has been observed *in vitro* and *in vivo* in other tumor model systems (24–26).

Several mechanisms underlying the antineoplastic activity of $1\alpha,25(OH)_2D_3$ have been proposed. Differences between tumor models and experimental conditions used in various studies may explain the lack of a unifying hypothesis about the hormone mode of action. Discrepancy between the effects of $1\alpha,25(OH)_2D_3$ may be dependent on the cell type and microenvironment. We found that $1\alpha,25(OH)_2D_3$ inhibited the growth of SVECs inducing G_0/G_1 arrest accompanied by a reduction in cyclin D1

levels and an accumulation of p27, but such events are not observed SVECs transformed with vGPCR. Thus, stable knockdown of the receptor indicated that, at least in part, the antiproliferative actions of the hormone in SVEC-vGPCR are mediated through the VDR without altering cyclin D1 and p27 levels. In this regard, a novel mechanism of autophagy has been recently published to explain the inhibition of proliferation and death of human myeloid leukemia cells by $1\alpha,25(OH)_2D_3$ (27). Other lines of evidence have shown that the antiproliferative actions of $1\alpha,25(OH)_2D_3$ involved the activation of the VDR through the MAPK pathways and activator protein-1/p21waf1 up-regulation in human osteosarcoma cells (28) and other cell types (29).

In addition to the classical genomic effects mediated by the VDR, $1\alpha,25(OH)_2D_3$ regulates a number of intracellular signaling pathways that ultimately affect cellular growth, differentiation, and apoptosis and may cooperate with the classical genomic pathway to transactivate the VDR (2). On the other hand, it has been published that endothelial cells transformed by vGPCR strongly activates the nuclear factor-κB (NF-κB) pathway, and NF-κB activation is a hallmark of both human and experimental KS (30). Of interest, among these alternatives, in vGPCR cells, recent preliminary gene reporter assays indicate that 10 nM $1\alpha,25(OH)_2D_3$ down-regulates the expression of NF-κB (12 and 48 h). Also, participation of ERK1/2 and p38 MAPK was ruled out by the absence of changes in their phosphorylation status (Gonzalez Pardo, V., A. R. de Boland, and R. Boland, unpublished observations). More detailed investigations are required to elucidate the mechanism involved in the antiproliferative action of the hormone in SVECs and vGPCR endothelial cells.

In conclusion, we have demonstrated that $1\alpha,25(OH)_2D_3$ and its TX527 analog have antiproliferative effects on the growth of endothelial cells transformed by the vGPCR *in vitro* and *in vivo*, the VDR being part of the inhibitory mechanism of action. In addition, the lack of superagonist activity of TX527 *in vivo* can be related to differences in its binding to Vitamin D binding protein compared with the natural hormone (22).

Acknowledgments

We thank Drs. Horacio Maturi, Graciela Gigola, and Guillermina Gomez for assistance in immunohistochemical analysis. The Fonds voor Wetenschappelijk Onderzoek (Grants 0553.06 and 0587.09) is gratefully acknowledged.

Address all correspondence and requests for reprints to: Drs. Ana Russo de Boland and Ricardo Boland Departamento Biología Bioquímica & Farmacia, Universidad Nacional del Sur, San Juan 670, 8000 Bahía Blanca, Argentina. E-mail: aboland@criba.edu.ar; or rboland@criba.edu.ar.

This work was supported by grants from Agencia Nacional de Promoción Científica y Tecnológica, Consejo Nacional de Investigaciones Científicas y Tecnológicas, and Universidad Nacional del Sur and Fulbright Scholar Program 2007.

Disclosure Summary: V.G.-P., D.M., J.S.G., A.V., A.R.d.B., and R.L.B. have nothing to disclose. R.B. has a license to a university patent and potential royalties for TX527 analog.

References

1. **DeLuca H** 2008 Evolution of our understanding of vitamin D. Nutr Rev 10:S73–S87
2. **Beer TM, Myrthue A** 2004 Calcitriol in cancer treatment: from the lab to the clinic. Mol Cancer Ther 3:373–381
3. **Norman AW, Nemere I, Zhou LX, Bishop JE, Lowe KE, Maiyar AC, Collins ED, Taoka T, Sergeev I, Farach-Carson MC** 1992 $1,25(OH)_2$-vitamin D_3, a steroid hormone that produces biologic effects via both genomic and nongenomic pathways. J Steroid Biochem Mol Biol 41:231–240
4. **Boland R, de Boland AR, Marinissen MJ, Santillan G, Vazquez G, Zanello S** 1995 Avian muscle cells as targets for the secosteroid hormone 1,25-dihydroxy-vitamin D3. Mol Cell Endocrinol 114:1–8
5. **Verlinden L, Eelen G, Van Hellemont R, Engelen K, Beullens I, Van Camp M, Marchal K, Mathieu C, Bouillon R, Verstuyf A** 2007 $1\alpha,25$-Dihydroxyvitamin D_3-induced down-regulation of the checkpoint proteins, Chk1 and Claspin, is mediated by the pocket proteins p107 and p130. J Steroid Biochem Mol Biol 103:411–415
6. **Bouillon R, Carmeliet G, Verlinden L, van Etten E, Verstuyf A, Luderer HF, Lieben L, Mathieu C, Demay M** 2008 Vitamin D and human health: lessons from vitamin D receptor null mice. Endocr Rev 29:726–776
7. **Masood R, Nagpal S, Zheng T, Cai J, Tulpule A, Smith DL, Gill PS** 2000 Kaposi sarcoma is a target for vitamin D3 receptor agonist. Blood 96:3188–3194
8. **Memar OM, Rady PL, Tyring SK** 1995 Human herpesvirus 8: detection of novel herpesvirus-like DNA sequences in Kaposi's sarcoma and other lesions. J Mol Med 73:603–609
9. **Whitby D, Howard MR, Tenant-Flowers M, Brink NS, Copas A, Boshoff C, Hatzioannou T, Suggett FE, Aldam DM, Denton AS** 1995 Detection of Kaposi sarcoma associated herpesvirus in peripheral blood of HIV-infected individuals and progression to Kaposi's sarcoma. Lancet 346:799–802
10. **Montaner S, Sodhi A, Molinolo A, Bugge TH, Sawai ET, He Y, Li Y, Ray PE, Gutkind JS** 2003 Endothelial infection with KSHV genes *in vivo* reveals that vGPCR initiates Kaposi's sarcomagenesis and can promote the tumorigenic potential of viral latent genes. Cancer Cell 3:23–36
11. **Grisotto MG, Garin A, Martin AP, Jensen KK, Chan P, Sealfon SC, Lira SA** 2006 The human herpesvirus 8 chemokine receptor vGPCR triggers autonomous proliferation of endothelial cells. J Clin Invest 116:1264–1273
12. **Pardo VG, Boland R, de Boland AR** 2006 $1\alpha,25(OH)$2-vitamin D3 stimulates intestinal cell p38 MAPK activity and increases c-*fos* expression. Int J Biochem Cell Biol 38:1181–1190
13. **Bradford MM** 1976 A rapid and sensitive method for quantification of micrograms quantities of proteins utilizing the principle of protein biding. Anal Biochem 72:248–254
14. **Gocek E, Kielbiński M, Marchinkowska E** 2007 Activation of intracellular signaling pathways is necessary for an increase in VDR expression and its nuclear translocation. FEBS Lett 581:1751–1757
15. **Eelen G, Verlinden L, Van Camp M, Claessens F, De Clercq P, Vandewalle M, Bouillon R, Verstuyf A** 2005 Altered vitamin D

receptor-coactivator interactions reflect superagonism of vitamin D analogs. J Steroid Biochem Mol Biol 97:65–68
16. **Chung I, Wong MK, Flynn G, Yu WD, Johnson CS, Trump DL** 2006 Differential antiproliferative effects of calcitriol on tumor-derived and matrigel-derived endothelial cells. Cancer Res 66:8565–8573
17. **Yang TY, Chen SC, Leach MW, Manfra D, Homey B, Wiekowski M, Sullivan L, Jenh CH, Narula SK, Chensue SW, Lira SA** 2000 Transgenic expression of the chemokine receptor encoded by human herpesvirus 8 induces an angioproliferative disease resembling Kaposi's sarcoma. J Exp Med 191:445–454
18. **Guyton KZ, Kensler TW, Posner GH** 2003 Vitamin D and vitamin D analogs as cancer chemopreventive agents. Nutr Rev 61:227–238
19. **Johnson CS, Hershberger PA, Bernardi RJ, McGuire TF, Trump DL** 2002 Vitamin D receptor: a potential target for intervention. Urology 60:123–130; discussion 130–131
20. **Eelen G, Gysemans C, Verlinden L, Vanoirbeek De Clercq EP, Van Haver D, Mathieu C, Bouillon R, Verstuyf A** 2007 Mechanism and potential of the growth-inhibitory actions of vitamin D and analogs. Curr Med Chem 14:1893–1910
21. **Bouillon R, Verlinden L, Eelen G, De Clercq P, Vandewalle M, Mathieu C, Verstuyf A** 2005 Mechanisms for the selective actions of vitamin D analogs. J Steroid Biochem Mol Biol 97:21–30
22. **Verlinden L, Verstuyf A, Van Camp M, Marcelis S, Sabbe K, Zhao XY, De Clerq P, Vandewalle M, Boullion R** 2000 Two novel 14-epi-analogues of 1,25-dihydroxyvitamin D3 inhibit the growth of human breast cancer cells *in vitro* and *in vivo*. Cancer Res 60:2673–2679
23. **Deeb KK, Trump DL, Johnson CS** 2007 Vitamin D signalling pathways in cancer: potential for anticancer therapeutics. Nat Rev Cancer 7:684–700
24. **Furigay P, Swamy N** 2004 Anti-endothelial properties of 1,25-dihydroxy-3-epi-vitamin D_3, a natural metabolite of calcitriol. J Steroid Biochem Mol Biol 89–90:427–431
25. **Mantell DJ, Owens PE, Bundred NJ, Mawer EB, Canfield AE** 2000 1α,25-Dihydroxyvitamin D_3 inhibits angiogenesis *in vitro* and *in vivo*. Circ Res 87:214–220
26. **Iseki K, Tatsuta M, Uehara H, Iishi H, Yano H, Sakai N, Ishiguro S** 1999 Inhibition of angiogenesis as a mechanism for inhibition by 1α-hydroxyvitamin D_3 and 1,25-dihydroxyvitamin D_3 of colon carcinogenesis induced by azoxymethane in Wistar rats. Int J Cancer 81:730–733
27. **Wang J, Lian H, Zhao Y, Kauss MA, Spindel S** 2008 Vitamin D3 induces autophagy of human myeloid leukemia cells. J Biol Chem 283:25596–25605
28. **Wu W, Zhang X, Zanello LP** 2007 1α,25-Dihydroxyvitamin D3 antiproliferative actions involve vitamin D receptor-mediated activation of MAPK pathways and AP-1/p21(waf1) up-regulation in human osteosarcoma. Cancer Lett 254:75–86
29. **Densham RM, Todd DE, Balmanno K, Cook SJ** 2008 ERK1/2 and p38 cooperate to delay progression through G_1 by promoting cyclin D1 protein turnover. Cell Signal 20:1986–1994
30. **Martin D, Galisteo R, Ji Y, Montaner S, Gutkind JS** 2008 An NF-κB gene signature contributes to Kaposis's sarcoma virus vGPCR-induced direct and paracrine neoplasia. Oncogene 27:1844–1852